Sneaker Male Squid Produce Long-lived Spermatozoa by Modulating Their Energy Metabolism

Noritaka Hirohashi[‡1*], Miwa Tamura-Nakano[§*], Fumio Nakaya[¶], Tomohiro Iida[‡], Yoko Iwata[†]

From the [‡]Oki Marine Biological Station, Education and Research Center for Biological Resources, Shimane University, Oki, 685-0024, Japan, [§]Research Institute, National Center for Global Health and Medicine, Tokyo, 162-8655, Japan, [¶]Center for Science Education, Osaka kyoiku University, Osaka 582-858, Japan, and [†]Atmosphere and Ocean Research Institute, University of Tokyo, Chiba, 277-8564, Japan

Running title: Sperm longevity in male dimorphism

[1]To whom correspondence should be addressed: Dr. Noritaka Hirohashi, Oki Marine Biological Station, Education and Research Center for Biological Resources, Shimane University, Oki, 685-0024, Japan, Telephone: +81-8512- 2-1814; FAX: +81-8512- 2-4357; E-mail: hiro@life.shimane-u.ac.jp
*These authors contributed equally to this work

Keywords: alternative reproductive tactics, postcopulatory sexual selection, male dimorphism, sperm metabolism, cephalopods

ABSTRACT
Spermatozoa released by males should remain viable until fertilization. Hence, sperm longevity is governed by intrinsic and environmental factors in accordance with male mating strategy. However, whether intraspecific variation of insemination modes can impact on sperm longevity remains to be elucidated. In the squid, *Heterololigo bleekeri*, male dimorphism (consort and sneaker) is linked to two discontinuous insemination modes that differ in place and time. Notably, only sneaker male spermatozoa inseminated long before egg spawning can be stored in the seminal receptacle. We found that sneaker spermatozoa exhibited greater persistence in fertilization competence and flagellar motility than consort ones owning to larger amount of flagellar glycogen. Sneaker spermatozoa also showed higher capacities in glucose uptake and lactate efflux. Lactic acidosis was considered to stabilize CO_2-triggered self-clustering of sneaker spermatozoa, thus establishing hypoxia-induced metabolic changes and sperm survival. These results, together with comparative omics analyses, suggest that postcopulatory reproductive contexts define sperm longevity by modulating the inherent energy levels and metabolic pathways.

Sperm traits can evolve through postcopulatory contexts involving sperm competition, cryptic female choice and insemination/fertilization environments. As consequences of sperm competition (1,2) and cryptic female choice (3,4), male individuals of certain species have evolved to produce giant spermatozoa to achieve better fertilization success. Besides morphological traits, the evolutionary forces driven by postcopulatory sexual selection should also favor more effective sperm motility and hence influence their morphological and energetic traits (5), thus facilitating fertilizations in polyandrous mating systems. Sperm competition theory predicts that an increased risk of sperm competition (sometimes referred to as female

promiscuity) should result in selection for increased sperm swimming velocity. A growing body of evidence has supported this prediction: thus, a positive relationship between sperm swimming speed and sperm competitiveness was seen not only in external fertilizers such as fish (6-8) but also in internal fertilizers such as birds (9,10) and mammals (11). Commonly, polyandrous insemination can occur simultaneously (external fertilization) or sequentially (internal fertilization) toward the same set of eggs. However, in species that employ internal fertilization, female individuals often store spermatozoa in their reproductive tract and use them during multiple ovulation cycles (12-14). Thus, it is possible that spermatozoa with greater longevity might have greater reproductive fitness than those with increased velocity. This implicates that spermatozoa should be able to modulate their energy expenditure adequately depending on the post-mating contexts.

The coastal squid, *Heterololigo bleekeri*, exhibits alternative male mating tactics in which complex polyandrous inseminations occur at different places and/or different occasions (15) (Fig. 1). In one scenario, promiscuous copulations by both sneaker and consort males occur just prior to egg spawning, so that the durations between sperm insemination and fertilization are short. In the other scenario, "sneaker" males copulate with females at much earlier times before egg spawning. Thereafter, their spermatozoa inseminated at the buccal membrane of the female migrate to the seminal receptacle and survive for an extended duration such as days or even months (16,17). In theory, because the mating opportunities for sneaker males are limited by the continuing presence of "consort" males, they should produce long-lived sneaker spermatozoa, whereas, consort males can make short-lived spermatozoa with a minimum need for energy shortage. In fact, sneaker spermatozoa require flagellar motility on two separate occasions: upon ejaculation from the spermatangium (when swimming toward the seminal receptacle) and after release from the seminal receptacle (when swimming toward the eggs). Furthermore, adenosine triphosphate (ATP) is thought to be required for cellular homeostasis to maintain the remarkable longevity of quiescent spermatozoa in the seminal receptacle (18). Thus, sneaker spermatozoa are, in general, more costly than consort ones in terms of the total amount of energy required for accomplishing fertilization. In this context, we speculated that sneaker spermatozoa would have expanded their metabolic system allowing on-demand energy production and storage (12). In the present study, we conducted comparative analyses between sneaker and consort male squid in term of sperm metabolism and related functions such as motility, longevity, and sustainability of fertilizing competence.

RESULTS

Sneaker spermatozoa exhibit longer fertilization competence than consort spermatozoa—We demonstrated previously that in *H. bleekeri,* both sneaker and consort male individuals produce euspermatozoa that are distinguishable from each other in morphological (flagellar length) and behavioral (self-swarming) properties (19,20). Although they are both fertilization-competent, we noted that sneaker spermatozoa exhibited greater fertilization success than consort spermatozoa when inseminated *in vitro* (19). We, therefore, investigated if they would exhibit different sustainability in fertilization competence. Spermatozoa released freshly from the spermatangium were recovered and stored in isolation from the spermatangia. An aliquot of the sperm suspension was used for IVF with mature oocytes at given time points. The data clearly showed that although higher fertilization rates were obtained in both types of sperm shortly after recovery from the spermatangium, fertilization competence was lost within 20 min in consort spermatozoa, whereas it remained unchanged for 45 min in sneaker spermatozoa (Fig. 2A). We further examined sneaker spermatozoa recovered from the seminal receptacle, the female's sperm storage organ. The fertilization

rates—although individual variation was remarkably high presumably due to differences in duration of sperm storage —represented values intermediate between the two sperm preparations described above (Fig. 2A).

We next conducted time-course measurements of the curvilinear velocity (VCL) with sperm diluted with seawater (approximately 10^6 cells/mL; dilution factor of 100 or DF100; Fig. 2B). We found that the rate of decrease in VCL was higher in consort spermatozoa with the average time required for VCL to decline by 100 μm/s (TRD100) was 5 min, n = 3) than with sneaker spermatozoa (TRD100; 30 min, n = 3). Moreover, the rate of decrease in VCL was accelerated by addition of the mitochondrial uncoupler CCCP to a greater extent in consort spermatozoa (TRD100: 1 min, n = 3) than in sneaker ones (TRD100: 5 min, n = 3). In addition, when glucose was added, both sneaker and consort spermatozoa maintained motility with a higher VCL (> 100 μm/s) for at least 40 min. These data suggest that although both oxidative phosphorylation (OXPHOS) and glycolytic pathways contributed to flagellar motility of both types of spermatozoa, the OXPHOS pathway plays major roles in the motility of consort spermatozoa.

To ascertain whether CCCP targets the mitochondria of squid spermatozoa immediately, the mitochondrial membrane potential ($\Delta\psi_m$) was monitored with a fluorescent indicator, JC-1 (Fig. 2C). In both types of spermatozoa, JC-1 fluorescence disappeared within 1 min after CCCP administration. In addition, CCCP had little effect on sperm intracellular pH (Fig. S1). Nonetheless, these JC-1-labeled spermatozoa exhibited normal motility (Fig. 2D), confirming that CCCP blocked mitochondrial ATP synthesis without affecting flagellar motility. Before addressing the detailed mechanisms of OXPHOS-dependent or independent pathways for flagellar motility, we examined the effect of sperm dilution, another factor influencing sperm longevity in marine broadcast spawners (21).

Sneaker spermatozoa in clusters sustain their longevity through anaerobic respiration—Relationships between sperm longevity (swimming lifetime) and sperm concentrations were investigated. Kinetic analysis revealed that the rate of decrease in VCL was constant at any sperm concentration in consort spermatozoa (Fig. 3A); however, in sneaker spermatozoa, the VCL was maintained at higher levels with less dilution for at least 40 min (Fig. 3B). Because higher concentrations of sperm could lead to hypoxia that will limit OXPHOS, the results indicated that only sneaker spermatozoa were able to change their respiration mode depending on sperm density.

To test this hypothesis, sperm suspensions diluted at DF100 were subjected to various hypoxic conditions (0.1% – 90% O_2 in air) for 1 h followed by VCL analysis. We found that hypoxia had no impact on sperm longevity for consort spermatozoa, whereas loss of VCL was significantly attenuated with lower oxygen concentrations for sneaker spermatozoa (Fig. 3C). Furthermore, incubation of consort spermatozoa with 1 μM CCCP resulted in a substantial decrease in motility after 30 min and a complete loss after 2 h regardless of sperm concentration (Fig. 2D). By contrast, in sneaker spermatozoa, this CCCP-induced loss of motility did not occur when a higher concentration of sperm (DF5) was used (Fig. 2D). Finally, we tested whether self-clustering—a trait specific for sneaker spermatozoa—could increase their longevity by increasing the local sperm density. Self-clustering was blocked with 2 mM ATZ (Fig. 3E), and thereafter VCL was measured during the next 2 h. We found that spermatozoa in clusters sustained their longevity, while those blocked from clustering showed reduced motility over time (Fig. 3F). Taken together, these results suggest that a reduction in oxygen level could change the respiratory mode from aerobic to anaerobic, with an impact on sperm longevity. We next searched for endogenous energy reserves that could sustain initial flagellar movement.

Glycogen serves as the major energy

source for initial motility persistence in sneaker spermatozoa—Previously, our comparative proteomic analysis identified that spermatozoa from consort males were preferentially loaded with many glycolytic and mitochondrial enzymes as well as glycogen-related enzymes such as phosphoprotein phosphatase 1 and phosphoglucomutase 1 (22). In addition, integrated *in silico* analysis of this proteome database with the KEGG PATHWAY (http://www.genome.jp/kegg/pathway.html) identified glycogenin-1, the primer for glycogen synthesis, that is more abundant in sneaker than in consort spermatozoa (S/C = 3.1–3.9, Figs S2A, B). Taken together, we predicted that glycogen metabolism might differ between sneaker and consort spermatozoa. First, paraffin wax sections of spermatangia were subjected to periodic acid-Schiff (PAS)-stain that detects polysaccharides including glycogen. We found that the spermatangia from sneaker males exhibited greater PAS-positivity than those from consort males (Figs 4A–D). We next measured glycogen levels in isolated spermatozoa and found that sneaker spermatozoa (27.5 ± 1.7 ng/cell, n = 3) stored glycogen at significantly greater levels than consort spermatozoa (3.2 ± 4.1 ng/cell; n = 3, Fig. 4E). The levels of intracellular glycogen decreased after leaving sperm suspensions in a diluted condition for 40 min (sneakers 4.9 ± 1.5 ng/cell; consorts 2.8 ± 1.6 ng/cell, Fig. 4E). These results indicate that sneaker spermatozoa exhibit facilitated energy metabolism greater than consort sperm not only in glycogen-storing capacity but also at energy consumption rate (~50-fold).

Studies with scanning (Fig. 4F) and transmission (Figs 4G, H) electron microscopy (TEM) identified well-compartmented organelles in both types of spermatozoa, especially in mitochondria that are located separate from the flagellum. Notably, relatively uniformly-sized granules (diameter 21.1 ± 0.4 nm, n = 53) with higher electron density, typical of β-glycogen particles, appeared in the cytoplasm of the flagellum, mitochondrial intermembrane space and underneath the plasma membrane overlying the sperm head (Fig. 4I, *arrowheads*, Fig. S3A). These results suggest that initial motility is driven by glycolysis following glycogen breakdown. Thus, the longer swimming lifetime in sneaker spermatozoa (in the order of hours) than in consort spermatozoa (> 1 h) can be explained by a difference in glycogen storage. However, sneaker spermatozoa should have a more extended lifespan such as days to weeks to participate in fertilization (Fig. 1).

Both sneaker and consort spermatozoa can use extracellular glucose to sustain motility, but only sneaker spermatozoa preferentially efflux D-lactate—Based on the results above, we hypothesized that additional energy sources, such as extracellular glucose, can produce ATP to drive flagellar motility, as known for *Loligo pealii* (23). We found in *H. bleekeri* that both types of spermatozoa exhibited sustained motility in glucose-containing seawater (Figs 2B, 5A) and continued swimming for up to 4 days (data not shown). Non-nutritional sugars and other glycolytic metabolites, except for D-lactate, had no significant effects on the sustainability of flagellar motility (Fig. 5A). Furthermore, sperm suspensions diluted in glucose-free seawater (such as DF100) lost motion within 2 h; thereafter, when treated with 1 mM glucose, both sneaker and consort spermatozoa become vigorously motile (Figs 5B, 5C). This glucose-induced recovery from loss of motility was severely attenuated by coincubation with 10 mM 2-deoxyglucose (2DG), a glycolytic inhibitor (Fig. 5C).

To confirm that the spermatozoa from both types of male squid are capable of glucose uptake, we carried out 2DG uptake experiments (Fig. 5D), where a greater capacity of glucose uptake was observed in sneaker spermatozoa (60.5 ± 1.9 nmols/cell/h, n = 3) than in consort spermatozoa (24.7 ± 3.2 nmols/cell/h, n = 3). In contrast, both types of sperm suspension were stimulated to undergo aerobic respiration by glucose to similar levels as determined by the rate of O_2 consumption (Fig. 5E). Thus, considering the difference in overall metabolic balance between sneaker and consort spermatozoa, the former types must deal with intracellular

accumulations of glucose metabolites such as pyruvate or lactate. In this context, we measured lactate efflux and found that in the absence of extracellular glucose (galactose was added as a control), there was no significant increase in D/L-lactate content in seawater (Fig. 5F). However, when glucose was added, the rate of D-lactate efflux was much greater in sneaker than in consort spermatozoa (Fig. 5F). These results suggest that glucose uptake can lead to sustained motility through glycolysis and OXPHOS in both types of spermatozoa, however only sneaker spermatozoa can show facilitated efflux of D-lactate (Fig. 5F, *bottom panels*).

Through comparison analysis using previously constructed database from RNA-seq and proteomics (22), we found that transcripts similar to the gene for glucose transporter 1 (*GLUT-1*), controlling glucose uptake into cells, were more abundantly expressed in sneaker than in consort testes (Fig. S2C). This result was supported by sperm proteome analysis, where peptides corresponding to GLUT-1 and hexokinase-4 were found to be more (4-fold) abundant in sneaker than in consort spermatozoa (Fig. S2B). Furthermore, monocarboxylate transporter 3/4 (*MCT3/4*), a putative lactate exporter, exhibited much greater expression (3-fold) in sneaker than in consort testes, whereas other members of the MCT gene family showed no biased expression (Fig. S2D). Together, these data suggest that sneaker spermatozoa are facilitated in long-term glycolysis independent of aerobic utilization of pyruvate by the Krebs cycle.

The seminal receptacle might protect stored sperm from glycogen depletion—We next searched potential sites for nutrition supply. We assayed for D-lactate, the end product of the glycolytic pathway rather than for unknown nutrient substances because the methodology is easy and endogenous glycogen does not significantly contribute to the production of D-lactate (Fig. 5F). In the spermatangium fluid, 7.13 ± 2.10 mg/mL (n = 3) and 2.61 ± 0.83 mg/mL (n = 3) of D-lactate were detected in sneaker and consort individuals, respectively. More remarkably, the seminal fluid recovered from the female seminal receptacle contained D-lactate at 11.76 ± 1.11 mg/mL (n = 3). However, it remains to be determined where exactly this is produced (see Discussion).

After being released from the seminal receptacle, sneaker spermatozoa must swim to reach an oocyte. We asked if spermatozoa in the seminal receptacle could still store some glycogen. For this, the numbers of glycogen granules were counted on TEM images of thin sections of sperm-containing specimens. In controls, when freshly isolated spermatangia were examined, the granules were much more abundant in sneaker males (Fig. 6A; 16.13 ± 0.42, n = 329) than in consort ones (Fig. 6D; 6.30 ± 0.28, n = 229). When sperm suspensions were incubated for 18 h, most granules disappeared for sneakers (Fig. 6B; 0.11 ± 0.07, n = 145) and for consorts (Fig. 6E; 0.20 ± 0.06, n = 134). However, when coincubated with 1 mM glucose, more glycogen granules were retained in sneaker spermatozoa (Fig. 6C; 4.32 ± 0.31, n = 233) but not in consort ones (Fig. 6F; 0.35 ± 0.10, n = 158), suggesting that sneaker spermatozoa can avoid glycogen shortage or replenish their glycogen contents in a nutrient-rich environment. Finally, we tested spermatozoa stored in seminal receptacles and found that glycogen remained to some extent (Fig. 6G; 1.89 ± 0.16, n = 281), suggesting that storage in the seminal receptacle also prevents spermatozoa from complete depletion of this intrinsic energy source.

We then evaluated which part of the flagellum is involved in glycogen granule storage. To understand the subcellular distribution of energy sources, cross-sectional images of the flagella were first categorized into three parts; near the basal body, around the central region and near the tail end as judged by the presence or absence of mitochondria in the same section and/or outer dense fibers (24) surrounding the axoneme (Figs 6H, S2). In sneaker spermatozoa stored in the spermatangium, glycogen granules were equally distributed in the entire flagellum except for the region proximal to the basal body. By contrast, for sneaker spermatozoa held in the seminal

receptacle, glycogen granules only appeared in the central region of the flagellum (Fig. 6I).

Sperm clusters are stabilized in a nutrient-rich environment—Previously, we found that spermatozoa from sneaker males exhibit self-clustering behavior caused by chemotaxis to respiratory CO_2 (20,25). The chemoreceptor for CO_2 is a membrane-anchored carbonic anhydrase (CA) that catalyzes the following reaction:
$CO_2 + HO \leftrightarrows HCO_3^- + H^+$

Protons produced through this reaction are the actual chemoattractants, so a proper proton gradient, created naturally or experimentally in the microenvironment, can lead to the formation of sperm clusters (20). Considering the facilitated lactate efflux from sneaker spermatozoa and rapid conversion into protons, we hypothesized that lactic acidosis might enhance sperm clustering. To test this, we used a semi-closed microchamber that allows quantitative analysis of the self-assembling/disassembling processes (Figs 7A, S3). When glucose and a CA inhibitor, ATZ were simultaneously added to sneaker spermatozoa, clusters did not form (Fig. 7A, *right end*), suggesting that the CA-mediated acidosis is necessary to establish the sperm cluster. Next, when the sperm clusters were first allowed to form, thereafter ATZ added (Fig. 7B), the clusters initiated disassembling immediately, and the remaining clusters became significantly smaller after 5 min (Figs 7C, D). These results suggest that if extracellular glucose is absent, CA-mediated acidification plays an essential role in both the establishment and the maintenance of sperm clusters. However, if glucose is present, the sperm clusters—once established—were maintained even after blocking CA-mediated acidification, supporting our hypothesis that glucose-dependent lactate efflux reinforces the sperm cluster formation.

DISCUSSION

During the spermatophoric reaction (23), spermatozoa of the squid *H. bleekeri* released from the spermatangium become motile immediately. Our previous observations revealed that, even after ejaculation, sneaker spermatozoa do not freely diffuse into seawater, instead preferentially stay in the vicinity of the ejaculatory duct of the spermatangium by forming a cluster (25). This phenomenon is absent in consort spermatozoa and can be explained by sneaker-specific sperm chemotaxis in response to self-emitted CO_2 (20). The physiological role of this clustering trait in sneaker spermatozoa remains to be determined, however, a sharp contrast in swimming behavior between sneaker and consort spermatozoa led us to examine the relationship between sperm concentration and sperm viability. We found that sneaker spermatozoa are capable of increasing their longevity by modulating their respiratory mode in response to sperm density. Lactate efflux enhanced the sperm cluster stability even after blocking the CA-mediated pathway (Fig. 7). Thus, this change in metabolic mode can enhance cell survival through a negative feedback mechanism. Currently, the intrinsic and environmental factors that control this respiratory mode remain unknown. In general, oxygen concentrations determine a cell's dependence on OXPHOS, known as the Pasteur effect. In fact, giant Pacific octopus (*Enteroctopus martini*) spermatozoa show an efflux of D-lactate when subjected to anaerobic conditions (26). However, recent studies on tumorigenesis have shed light on aerobic glycolysis (Warburg effect), where enhanced glucose uptake and lactate efflux can occur under normoxic conditions in solid tumors (27,28). Aerobic glycolysis might explain, at least in part, why sneaker spermatozoa are capable of a constant efflux of lactate even when the initial oxygen concentration is high (Figs 5D, F). In mammals, lactate produced from Sertori cells in the testis is able to nourish developing germ cells for survival and development (29,30). In the squid, D-lactate, but not L-lactate, maintained the motility of only sneaker spermatozoa to some extent (Fig. 5A). Because high concentrations of lactate were detected in the seminal receptacle, this metabolite might help to sustain sperm survival under

anaerobic conditions (31).

In mammals, spermatozoa are ejaculated into the female reproductive tract together with accessory gland secretions that contain fructose from the seminal vesicles for sperm nutrition (32). Similarly, nutrition supply to sneaker squid spermatozoa might occur in the spermatophore and/or in the seminal receptacle. Although mammalian spermatozoa are also capable of ATP generation through glycolysis and OXPHOS in the flagellum and mitochondria, respectively, sperm glycolysis plays a pivotal role in fertility (33-35). Nonetheless, how much and at which point mitochondrial ATP synthesis contributes to mammalian male fertility remain unknown (36).

Storing of spermatozoa in the female tract for certain times is a widespread phenomenon throughout animal phyla from insects to mammals (14). In these systems, spermatozoa are required to survive in a quiescent state. A large amount of ATP is generated to propel flagellar motility; however, quiescent cells in storage should require only low levels of ATP to maintain cellular metabolism and homeostasis (18). In *H. bleekeri*, spermatozoa from sneaker males are capable of being stored in the female seminal receptacle. We found that only these sperm types could efficiently change their mode of respiration. Sperm concentrations strongly influence the respiratory mode, particularly OXPHOS-independent sperm survival, which probably represents a quiescent state for those stored in the seminal receptacle. In sea urchin spermatozoa, dilution from the raw semen evokes a respiratory burst (37), resembling the OXPHOS-dependent (CCCP-sensitive) motility initiation in squid sperm.

In general, spermatozoa once diluted have no intrinsic capacity of clustering with each other. In species employing internal fertilization systems, spermatozoa in some species can form clusters with mechanical cell-to-cell contact, which is regarded as a cooperative behavior in favor of moving faster in the female reproductive track (38). In the squids, spermatozoa from sneaker males exhibit a self-clustering trait even after individual cells have been separated. Because they are inseminated externally and yet moved to the seminal receptacle, self-clustering could be associated with postcopulatory event(s) specific to sneaker spermatozoa such as sustained longevity, migration to the seminal receptacle or switching their respiratory mode. Our current study, together with previous reports (19,20) suggests that there has been coordinated evolution of complex adaptive traits constrained by postcopulatory reproductive contexts. Future studies should address the molecular and cellular mechanisms of how squid spermatozoa are capable of storing glycogen at different levels. The physiological role of lactate efflux for sperm quiescence should also be considered in this species (31). These studies will open up new avenues in the field of andrology with the hope of developing treatments for human male infertility associated with flagellar motility deficiencies (39).

EXPERIMENTAL PROCEDURES

Sperm collection—Sneaker and consort male *H. bleekeri* were obtained from fisheries (Aomori city, Miura city and Oki-no-shima, Japan) as dead animals. Sneakers and consorts were distinguished by discrete dimorphism in their spermatophore length (19). They were dissected to recover the spermatophores, and these were stored in moist chambers at 4 °C. Spermatophores stimulate a "spermatophoric reaction" which discharges a spermatangium (sperm mass in an inner tunic) from the outer tunic (23). Spermatozoa become motile near the posterior opening of the spermatangium just before swimming out. Stimulated spermatangia were transferred into test tubes with 50–100 μL of chilled normal seawater and stood on ice for 5–30 min, depending on the experimental design. Sperm concentrations were determined using a hemocytometer. Composition of normal seawater was: 480 mM NaCl, 10 mM KCl, 27 mM $MgCl_2$, 29 mM $MgSO_4$, 10 mM $CaCl_2$, and 2 mM $NaHCO_3$ (pH 8.0).

In vitro fertilization assay—To quantify the fertilizing competence of the

spermatozoa ejaculated from the spermatophore, in vitro fertilization (IVF) assays were performed as described (19). Spermatophores were recovered from Needham's sac (male reproductive accessory organ, where mature spermatophores are stored) and were stimulated to discharge the spermatangium. Spermatozoa released from these were used for IVF assays. To obtain roughly equal numbers of ejaculated spermatozoa, five (for consort) or 20 (for sneaker) stimulated spermatophores were placed in a test tube containing 1 mL of seawater. Similarly, sperm suspensions were squeezed from the seminal receptacle of five female individuals, thereafter suspended in 1 mL of seawater. After 5 min, the supernatants were transferred into fresh test tubes and kept at room temperature. Mature oocytes were obtained from oviducts and placed in a 35-mm diameter Petri dish in the absence of seawater. Approximately 100 oocytes per dish were inseminated with 100–200 μL of sperm suspension followed by gentle stirring with a plastic spatula. Five minutes after insemination, the dishes were filled with seawater and kept at 12 °C. After 30 min, excess spermatozoa were removed and replaced with fresh seawater several times, followed by overnight incubation at 15 °C. Fertilization success was determined by the presence or absence of cleavage planes in the animal hemisphere of the egg. All eggs inseminated were scored using a stereomicroscope.

Sperm motility analysis—Sperm suspensions were emitted from the spermatangia into a small volume of seawater (10–30 μL) and stored on ice until use. Sperm concentration adjusted to ~10^8 cells/mL was defined as undiluted semen (dilution factor 1, DF1). The sperm suspension was placed into an observation chamber that consisted of a 0.2-mm thick silicon support with a 1-cm^2 cutout onto which a glass slide and a 1% bovine serum albumin-coated coverslip were attached. Sperm swimming velocity was measured using a Sperm Motility Analysis System (SMAS; Detect, Tokyo, Japan), which automatically tracks swimming spermatozoa under a microscope (TE-2000, Nikon, Tokyo, Japan) and calculates their motility parameters. The percentage of motile cells was calculated automatically using the SMAS. Curvilinear velocity (μm/sec) was obtained from the distance tracked along the sperm swimming path per second.

Comparative analysis of gene expression profile between sneaker and consort using omics database—The annotated datasets that have constructed from testis transcriptome (RNA-seq) and sperm proteome in the previous work (Yoshida et al. 2014) were searched for putative glucose transporters (GLUTs), lactate transporters, glycogen metabolic enzymes and glucose metabolic enzymes as diagramed in Fig. S2A. From proteomic dataset, peptide counts of each protein were compared between sneaker and consort sperm (Fig. S2B). From transcriptome dataset, relative amounts of transcripts for *GLUTs* and monocarboxylate transporter (*MCT*) family were compared between sneaker and consort (Figs S2C, D).

Analytical methods—Commercially available fluorometric assay kits were used to measure glycogen (EnzyChrom™; BioAssay Systems, Hayward, CA, USA) and D/L-lactate (Cayman Chemical, Ann Arbor, MI, USA) concentrations according to the manufacturers' protocols. Measurement of 2-deoxyglucose (2DG) uptake in spermatozoa was carried out using a colorimetric assay kit (Cosmo Bio Co. Ltd., Tokyo, Japan). To calculate the amount of 2DG uptake and lactate efflux per cell, sperm concentrations were measured by a hemocytometer after fixing an aliquot of the suspension in each experiment. Seminal fluids in the spermatangium were recovered in the supernatant after centrifugation (14,000 *g*, 30 min, 4 °C) of the minced spermatangium (10 spermatangium per sample) to remove sperm cells. Similarly, to collect seminal fluid from the female seminal receptacle, semen was first squeezed out from the single entrance, followed by centrifugation to remove sperm cells. The semen was pooled in one fraction from at least 40 individuals for a single measurement.

Concentrations of O_2 dissolved in a sperm suspension were monitored in an airtight microchamber (40 μL) using noninvasive optical sensors for oxygen (Fibox 3, PreSens – Precision Sensing GmbH, Regensburg, Germany). To prepare seawater with different hypoxic conditions, nitrogen gas was purged through normal seawater placed in the glass bottle and the oxygen concentration was monitored with this sensor. In all measurements, experiments were carried out at least three times using three different batches of male squid and the data were expressed as the mean ± SEM. The Mann–Whitney *U* tests were used to compare differences between group means, and differences were considered significant at $P < 0.05$.

JC-1 staining—To monitor the mitochondrial membrane potential ($\Delta\Psi_m$) of spermatozoa, a fluorescent probe, JC-1 (Thermo Fisher Scientific, Waltham, MA, USA) was used with a method previously applied to sea urchin spermatozoa (40) with a slight modification. Briefly, 1 μL of 3 mM JC-1 (in dimethyl sulfoxide; DMSO) was diluted with 99 μL of ultrapure (Milli-Q) water to make a stock solution that was kept on ice in the dark. For each experiment, 0.5 μL of the stock JC-1 solution was diluted with 49.5 μL of seawater, thereafter 10 μL of a sperm suspension was added and incubated at 20 °C for 20 min in the dark. A droplet (10 μL) of seawater containing either 1 mM glucose, 1 mM carbonyl cyanide *m*-chlorophenyl hydrazine (CCCP) or DMSO (mock control) was placed on a coverslip (60 × 24 mm) followed by addition of 1 μL JC-1-stained sperm. After overlaying with a coverslip (24 × 24 mm), spermatozoa were observed under an epifluorescence microscope with a filter set (excitation 488 nm/emission 510–560 nm) and a video camera (NEC-550b; NEC Corp., Tokyo, Japan).

PAS-staining for paraffin sections—Spermatangia were fixed with 4% formaldehyde and dehydrated with ethanol series and xylene series, immersed in paraffin wax and sectioned in 2 μm thickness. Sections were deparaffined, oxidized by 1% periodic acid for 15 min and stained with Schiff's reagent (Muto chemical, Tokyo, Japan) and counterstained with hematoxylin for 20 sec.

Quantitation of sperm cluster formation—A microchamber, consisting of two coverslips bridged by a 1 mm thick silicon plate with a 6 mm diameter hole, was filled with 25 μL of sperm suspension containing either 1 mM glucose or 1 mM galactose. The upper side of the chamber was left slightly open to allow the introduction of an additional test compound (5 μL). The chamber was set on a video microscope (Nikon TE-2000, NEC-R550 camera) and the progression of sperm cluster formation was recorded under halogen light. Acetazolamide (ATZ, final concentration 2 mM) or DMSO (final 1.2%) was added after 15 min of loading the sperm suspension, and video recording continued. The magnitude of cluster formation was quantified as follows. The conditions of video recording were adjusted so that the luminosity value represented sperm density. The luminance distribution (LD) in the images was measured using Image J software (http://imagej.nih.gov/ij/). At the beginning of sperm loading into the chamber, the LD was fitted to a Gaussian distribution. As a cluster developed, the LD became bipolarized so the standard deviation (SD) of the LD became larger. The SD value represented a non-linear relationship to the degree of cluster formation (Fig. S4). In addition, various patterns of sperm clusters appeared after 15 min, however, the SD reached similar values. Thus, we used the SD to represent the integrity of sperm clusters (arbitrary unit).

Electron microscopy—Spermatozoa or spermatangia were prefixed with 2.5% glutaraldehyde in 0.1 M sodium cacodylate buffer containing 0.45 M sucrose (pH 7.4) for 24 h at 4 °C (41), washed with 0.1 M sodium cacodylate buffer containing 0.45 M sucrose (pH 7.4) and were postfixed with 1% osmium tetroxide (OsO_4) and 10 mM potassium ferricyanide [$K_3Fe(CN)_6$] in 0.1 M sodium cacodylate buffer for 1 h at room temperature. After fixation, samples

were rinsed three times in Milli-Q water. These samples were used for scanning and transmission electron microscopies.

For scanning electron microscopy, fixed spermatozoa were dehydrated in a graded ethanol series and immersed in t-butyl alcohol, frozen and dried by a vacuum evaporator and coarted with carbon using a carbon coater (JEE-420T; JEOL, Tokyo, Japan). Samples were examined in an electron microscope (TM-3030; Hitachi, Tokyo, Japan).

For transmission electron microscopy, samples were centrifuged at 200 *g* for 5 min and enrobed in an agarose (final concentration ~1.5%) for easy handling. Agarose blocks containing the fixed spermatozoa/spermatangia were dissected into small pieces, dehydrated in a graded ethanol series and embedded in epoxy resin (Quetol 812; Nisshin EM Co. Ltd., Tokyo, Japan). Each sample was sectioned at 70-nm with an ultramicrotome (EM UC7; Leica, Wetzlar, Germany), and stained with uranyl acetate and lead citrate. Sections were examined in an electron microscope (JEM-1400; JEOL, Tokyo, Japan). The diameters of glycogen particles and cross-sectioned flagella were measured using Image J (Fig. S3).

Acknowledgements: We thank Eiichi Okumura, Manabu Yoshida, the technical staffs at Misaki Marine Biological Station (MMBS) and Japanese Association for Marine Biology (JAMBIO) for their support. We thank Tomohiro Sasanami for critical reading of the manuscript.

Conflict of interest: The authors declare no competing financial interests.

Author contributions: N.H. and Y.I. designed the experiments. N.H., M.T.N., T.I. and I.Y. performed the experiments. F.N. analyzed the data. N.H. wrote the paper.

REFERENCES

1. Parker, G. A. (1970) Sperm competition and evolutionary consequences in the insects. *Biol Rev* **45**, 525-567
2. Parker, G. A. (1993) Sperm competition games: sperm size and sperm number under adult control. . *Proc Biol Sci* **253**, 245-254
3. Thornhill, R. (1983) Cryptic Female Choice and Its Implications in the Scorpionfly *Harpobittacus nigriceps*. *Am Nat* **122**, 756-788
4. Miller, G. T., and Pitnick, S. (2002) Sperm-female coevolution in Drosophila. *Science* **298**, 1230-1233
5. Tourmente, M., Rowe, M., Gonzalez-Barroso, M. M., Rial, E., Gomendio, M., and Roldan, E. R. (2013) Postcopulatory sexual selection increases ATP content in rodent spermatozoa. *Evolution* **67**, 1838-1846
6. Burness, G., Casselman, S. G., Schulte-Hostedde, A. I., Moyes, C. D., and Montgomerie, R. (2004) Sperm swimming speed and energetics vary with sperm competition risk in bluegill (*Lepomis macrochirus*). *Behav Ecol Sociobiol* **56**, 65-70
7. Fitzpatrick, J. L., Montgomerie, R., Desjardins, J. K., Stiver, K. A., Kolm, N., and Balshine, S. (2009) Female promiscuity promotes the evolution of faster sperm in cichlid fishes. *Proc Natl Acad Sci U S A* **106**, 1128-1132
8. Gasparini, C., Simmons, L. W., Beveridge, M., and Evans, J. P. (2010) Sperm swimming velocity predicts competitive fertilization success in the green swordtail *Xiphophorus helleri*. *PLoS One* **5**, e12146
9. Kleven, O., Fossoy, F., Laskemoen, T., Robertson, R. J., Rudolfsen, G., and Lifjeld, J. T. (2009) Comparative evidence for the evolution of sperm swimming speed by sperm competition and female sperm storage duration in passerine birds. *Evolution* **63**,

2466-2473
10. Bennison, C., Hemmings, N., Slate, J., and Birkhead, T. (2015) Long sperm fertilize more eggs in a bird. *Proc Biol Sci* **282**, 20141897
11. Gomez Montoto, L., Varea Sanchez, M., Tourmente, M., Martin-Coello, J., Luque-Larena, J. J., Gomendio, M., and Roldan, E. R. (2011) Sperm competition differentially affects swimming velocity and size of spermatozoa from closely related muroid rodents: head first. *Reproduction* **142**, 819-830
12. Ribou, A. C., and Reinhardt, K. (2012) Reduced metabolic rate and oxygen radicals production in stored insect sperm. *Proc Biol Sci* **279**, 2196-2203
13. Sasanami, T., Matsuzaki, M., Mizushima, S., and Hiyama, G. (2013) Sperm storage in the female reproductive tract in birds. *J Reprod Dev* **59**, 334-338
14. Orr, T. J., and Brennan, P. L. (2015) Sperm storage: distinguishing selective processes and evaluating criteria. *Trends Ecol Evol* **30**, 261-272
15. Iwata, Y., Munehara, H., and Sakurai, Y. (2005) Dependence of paternity rates on alternative reproductive behaviors in the squid Loligo bleekeri. *Mar Ecol Prog Ser* **298**, 219-228
16. Drew, G. A. (1911) Sexual activities of the squid, *Loligo pealii* (Les.). *J Morphol* **22**, 327–359
17. Hanlon, R. T., Smale, M. J., and Sauer, W. H. H. (2002) The mating system of the squid *Loligo vulgaris reynaudii* (Cephalopoda, Mollusca) off South Africa: Fighting, guarding, sneaking, mating and egg laying behavior. *Bull Mar Sci* **71**, 331-345
18. Zhang, L., Yang, P., Bian, X., Zhang, Q., Ullah, S., Waqas, Y., Chen, X., Liu, Y., Chen, W., Le, Y., Chen, B., Wang, S., and Chen, Q. (2015) Modification of sperm morphology during long-term sperm storage in the reproductive tract of the Chinese soft-shelled turtle, *Pelodiscus sinensis*. *Sci Rep* **5**, 16096
19. Iwata, Y., Shaw, P., Fujiwara, E., Shiba, K., Kakiuchi, Y., and Hirohashi, N. (2011) Why small males have big sperm: dimorphic squid sperm linked to alternative mating behaviours. *BMC Evol Biol* **11**, 236
20. Hirohashi, N., Alvarez, L., Shiba, K., Fujiwara, E., Iwata, Y., Mohri, T., Inaba, K., Chiba, K., Ochi, H., Supuran, C. T., Kotzur, N., Kakiuchi, Y., Kaupp, U. B., and Baba, S. A. (2013) Sperm from sneaker male squids exhibit chemotactic swarming to CO_2. *Curr Biol* **23**, 775-781
21. Levitan, D. R., Sewell, M. A., and Chia, F. S. (1991) Kinetics of fertilization in the sea urchin Strongylocentrotus franciscanus: interaction of gamete dilution, age, and contact time. *Biol Bull* **181**, 371-378
22. Yoshida, M. A., Yamada, L., Ochi, H., Iwata, Y., Tamura-Nakano, M., Sawada, H., Sauer, W. H., Ogura, A., and Hirohashi, N. (2014) Integrative omics analysis reveals differentially distributed proteins in dimorphic euspermatozoa of the squid, *Loligo bleekeri*. *Biochem Biophys Res Commun* **450**, 1218-1224
23. Austin, C. R., Lutwak-Mann, C., and Mann, T. (1964) Spermatophores and Spermatozoa of the Squid Loligo Pealii. *Proc R Soc Lond B Biol Sci* **161** 143-152
24. Lindemann, C. B. (1996) Functional significance of the outer dense fibers of mammalian sperm examined by computer simulations with the geometric clutch model. *Cell Motil Cytoskeleton* **34**, 258-270
25. Hirohashi, N., and Iwata, Y. (2013) The different types of sperm morphology and behavior within a single species: Why do sperm of squid sneaker males form a cluster? *Commun Integr Biol* **6**, e26729
26. Mann, T., Martin, A. W., Thiersch, J. B., Lutwak-Mann, C., Brooks, D. E., and Jones, R. (1974) D(—)-Lactic Acid and D(—)-Lactate Dehydrogenase in Octopus Spermatozoa. *Science* **185** 453-454
27. Hirschhaeuser, F., Sattler, U. G., and Mueller-Klieser, W. (2011) Lactate: a metabolic key player in cancer. *Cancer Res* **71**, 6921-6925
28. Vander Heiden, M. G., Cantley, L. C., and Thompson, C. B. (2009) Understanding the Warburg effect: the metabolic requirements of cell proliferation. *Science* **324**,

1029-1033
29. Mita, M., and Hall, P. F. (1982) Metabolism of round spermatids from rats: lactate as the preferred substrate. *Biol. Reprod* **26**, 445-455
30. Boussouar, F., and Benahmed, M. (2004) Lactate and energy metabolism in male germ cells. *Trends Endocrinol. Metab.* **15**, 345–350
31. Matsuzaki, M., Mizushima, S., Hiyama, G., Hirohashi, N., Shiba, K., Inaba, K., Suzuki, T., Dohra, H., Ohnishi, T., Sato, Y., Kohsaka, T., Ichikawa, Y., Atsumi, Y., Yoshimura, T., and Sasanami, T. (2015) Lactic acid is a sperm motility inactivation factor in the sperm storage tubules. *Sci Rep* **5**, 17643
32. Mann, T. (1946) Studies of the metabolism of semen. 3. Furctose as a normal constituents of seminal plasma. Site of formation and function of fructose in semen. *Biochem J* **40**, 481–491
33. Mukai, C., and Okuno, M. (2004) Glycolysis plays a major role for adenosine triphosphate supplementation in mouse sperm flagellar movement. *Biol Reprod* **71**, 540-547
34. Miki, K., Qu, W., Goulding, E. H., Willis, W. D., Bunch, D. O., Strader, L. F., Perreault, S. D., Eddy, E. M., and O'Brien, D. A. (2004) Glyceraldehyde 3-phosphate dehydrogenase-S, a sperm-specific glycolytic enzyme, is required for sperm motility and male fertility. *Proc Natl Acad Sci U S A* **101**, 16501-16506
35. Storey, B. T. (2008) Mammalian sperm metabolism: oxygen and sugar, friend and foe. *Int J Dev Biol* **52**, 427-437
36. Nascimento, J. M., Shi, L. Z., Tam, J., Chandsawangbhuwana, C., Durrant, B., Botvinick, E. L., and Berns, M. W. (2008) Comparison of glycolysis and oxidative phosphorylation as energy sources for mammalian sperm motility, using the combination of fluorescence imaging, laser tweezers, and real-time automated tracking and trapping. *J Cell Physiol* **217**, 745-751
37. Christen, R., Schackmann, R. W., and Shapiro, B. M. (1983) Metabolism of sea urchin sperm. Interrelationships between intracellular pH, ATPase activity, and mitochondrial respiration. *J Biol Chem* **258**, 5392-5399
38. Moore, H., Dvorakova, K., Jenkins, N., and Breed, W. (2002) Exceptional sperm cooperation in the wood mouse. *Nature* **418**, 174-177
39. Amaral, A., Castillo, J., Estanyol, J. M., Ballesca, J. L., Ramalho-Santos, J., and Oliva, R. (2013) Human sperm tail proteome suggests new endogenous metabolic pathways. *Mol Cell Proteomics* **12**, 330-342
40. Bineta, M. T., Doyleb, C. J., Williamsonc, J. E., and Schlegelc, P. (2014) Use of JC-1 to assess mitochondrial membrane potential in sea urchin sperm. *J Exp Mar Biol Ecol* **452**, 91–100
41. Konno, A., Shiba, K., Cai, C., and Inaba, K. (2015) Branchial cilia and sperm flagella recruit distinct axonemal components. *PLoS One* **10**, e0126005

FOOTNOTES

The abbreviations used are: ATZ, acetazolamide; CA, carbonic anhydrase; CCCP, carbonyl cyanide m-chlorophenyl hydrazine; DF, dilution factor; 2DG, 2-deoxy glucose; GULT, glucose transporter; IVF, in vitro fertilization; LD, luminance distribution; MCT, monocarboxylate transporter; ODF, outer dense fiber; OXPHOS, oxidative phosphorylation; TEM, transmission electron microscopy; VCL, curvilinear velocity.

FIGURE LEGENDS

FIGURE 1. Time-course of postcopulatory events in ejaculates from sneaker and consort males in the squid *Heterololigo bleekeri.* Sneaker males attempt copulations at different time points of the female reproductive sequence: either long before (head-to-head) or just prior to (sneaking) egg spawning. Ejaculates prematurely inseminated need to be stored in the female seminal receptacle until used for fertilization. In contrast, consort males always copulate with females in synchrony with egg spawning (males in parallel). The duration of sperm storage in

the seminal receptacle is unknown. SM, spermatangium; SR, seminal receptacle

FIGURE 2. Kinetic correlation between fertilization competence and sperm velocity. *A*, the fertilizing competence of diluted sperm suspensions was investigated using in vitro fertilization (IVF) assays. In consort spermatozoa that were collected from spermatangia, there was a rapid decrease in the fertilization rate after dilution (*magenta*), whereas no significant decrease in fertilization competence was observed in sneaker spermatozoa collected from the spermatangia (*blue*). When sneaker spermatozoa collected from the female seminal receptacles were tested, the IVF rates showed intermediate values between the above two experiments (*cyan*). *B*, spermatozoa freshly recovered from spermatangia were diluted with seawater at a final concentration of ~10^6 cells/mL (dilution factor, DF100) containing 1% DMSO (mock), 1 μM CCCP (cccp) or 1 mM glucose (glc), followed by incubation at 20 °C. Sperm curvilinear velocity (VCL) was analyzed after the indicated time points (n = 3). (C) JC-1-labeled sperm suspensions were treated with 1% DMSO (mock), 1 μM CCCP (cccp) or 1 mM glucose (glc) and photographed after 1 min.

FIGURE 3. Sneaker spermatozoa show increased longevity under anaerobic conditions. *A* and *B*, sperm suspensions freshly recovered from spermatangia were subjected to a dilution factor (DF) series of 5–500 with seawater, then incubated at 20 °C. The sperm VCL was measured after the indicated time points. Insets show the VCL with various dilution factors after 30 min of incubation. *C*, sperm suspensions were diluted (DF100) with seawater containing different concentrations of dissolved oxygen (0.1–90% in air) followed by 1-h incubation in an airtight chamber. Thereafter, VCL was measured. *D*, sperm suspensions with two different DFs (5 or 100) were treated with 1 μM CCCP (cccp) or without (mock). *E*, as the result of self-clustering, the concentrated sperm mass appeared at the bottom of a test tube (mock), whereas 2 mM ATZ inhibited self-clustering (ATZ). *F*, kinetic analysis of sperm VCL values incubated with 2 mM ATZ (+ATZ) or without (mock).

FIGURE 4. Sneaker spermatozoa store glycogen as the major energy source for initial motility. *A–D*, representative images of sections from paraffin wax-embedded spermatangia after PAS staining. PAS-positive materials were enriched to a greater extent in sneaker spermatangia (*A, B*) than in consort spermatangia (*C, D*). Enlarged images are shown in (*B*) and (*D*). *E*, the levels of intracellular glycogen in sneaker (open bars) and consort (closed bars) spermatozoa before or at 40 min after dilution (n = 3). * $P < 0.05$. *F*, SEM image of a sneaker spermatozoon. *G–I*, TEM images of the axial- (*G*) and cross- (*H*) sections of sneaker spermatozoa. Key: Nuc, nucleus; Mito, mitochondria; Fla, flagellum. *I*, a cross-section of a spermatangium packed with sneaker spermatozoa. Nuclei, mitochondria, and flagella are shown in *blue*, *red* and *magenta*, respectively. Arrowheads (*cyan*) indicate glycogen granules. The numbers in each photograph indicate the length of scale bars in μm.

FIGURE 5. Sustainable motility depends on an energy supply from both inside and outside the spermatozoon. *A*, Sperm suspensions were diluted with seawater (DF100) containing the compounds as indicated at a final concentration of 1 mM. After 2 h of incubation, the percentages of motile spermatozoa were counted (n = 3). *B*, sperm suspensions were prepared in diluted conditions (DF100) for 2 h, thereafter the compound was added as indicated. The percentages of motile spermatozoa were counted 5 min after any addition. Closed bars, sneaker spermatozoa; open bars, consort spermatozoa. *C*, motility was measured after incubation with 1 mM glucose (*closed circles*), 1 mM galactose (*closed triangles*) or 1 mM glucose plus 20 mM 2-deoxyglucose (*open circles*). *D*, 2DG uptake by spermatozoa was measured (n = 3). * $P < 0.05$. *E*, the oxygen consumption rate was determined before (mock) and after (D-Glc) treatment with 1 mM glucose (n = 3). *F*, sperm suspensions (1×10^6 cells/mL) from consort or sneaker males were incubated in seawater containing 1 mM glucose (D-Glc) or 1 mM galactose (D-Gal). After the indicated time points, the supernatant from which sperm cells were removed by centrifugation was recovered after removing the spermatozoa by

centrifugation and assayed for the concentration of L-lactate or D-lactate. Data represent the mean ± SEM (n = 3).

FIGURE 6. Densities and distribution of glycogen granules in spermatozoa. *A–G*, Scatter plots show the numbers of glycogen granules (x-axis) along the flagellar axis (the diameter of an approximate circle of the corresponding flagellar cross-section; y-axis). Sneaker spermatozoa stored in the spermatangium (*A*) for 18 h were released into seawater in the absence (*B*) or presence (*C*) of 1 mM glucose. Parallel experiments with consort spermatozoa are shown in *D–F*. *G*, sneaker spermatozoa stored in the female seminal receptacle. *H*, *top*, an illustration of a spermatozoon indicates the approximate section positions (*tail*, near flagellar tail; *mid*, around middle part; *bas*, basal part) along the flagellar (A-T) axis. *Bottom*, Representative images of flagellar sections for the corresponding three regions. Key: G, glycogen granules; ODF, outer dense fiber. *I*, distribution of glycogen granules in the three regions of a flagellum. Spermatozoa in a sneaker spermatangium (Sn), a consort spermatangium (Cs) and a female seminal receptacle (Sr) were examined.

FIGURE 7. Lactate efflux promotes the maintenance of sperm clustering but not its establishment. *A*, time-lapse images (from *left* to *right*) during sperm cluster formation. Sperm cells that were evenly distributed (1 min) became concentrated with time and three major clusters (*white patches*) appeared after 15 min in this trial. Clustering did not occur if 1 mM glucose and 1 μM CCCP were present (*right end*). *B*, this diagram shows an experimental scheme to examine the sustainability of sperm clustering after blocking the CA-mediated chemotactic pathway with acetazolamide (ATZ). The order of addition to the observing chamber was glucose (or galactose as a negative control), sperm and ATZ (or DMSO as a solvent control). *C*, representative images of clusters assembling (*left*) in the presence of 1 mM glucose (Glc) or galactose (Gal) and clusters disassembling (*right*) 5 min after adding ATZ. *D*, quantification of sperm clustering (supplemental Fig S4) from panel *C* (n = 4). *White* and *gray* columns indicate before and 15 min after addition of ATZ (or DMSO), respectively. * $P < 0.05$.

FIGURE 8. Model of sperm metabolism and longevity control in squid spermatozoa. Sperm ATP can be generated from internal glycogen and external glucose through glycolysis and oxidative phosphorylation (Krebs cycle). Sneaker spermatozoa are more efficient than consort spermatozoa in terms of glycogen storage, glucose uptake, and lactate efflux, resulting in acidification of their microenvironment. In conjunction with emitted CO_2 this leads to sperm clustering. Spermatozoa in clusters survive for longer times because of limitations to flagellar motility and oxygen availability. The resulting hypoxia blocks the Krebs cycle and promotes lactate efflux. Thus, sperm clusters accumulate metabolic wastes that reduce energy consumption through negative feedback. Pathways and components labeled in *red* are better in sneaker than in consort spermatozoa (Sneaker > > Consort).

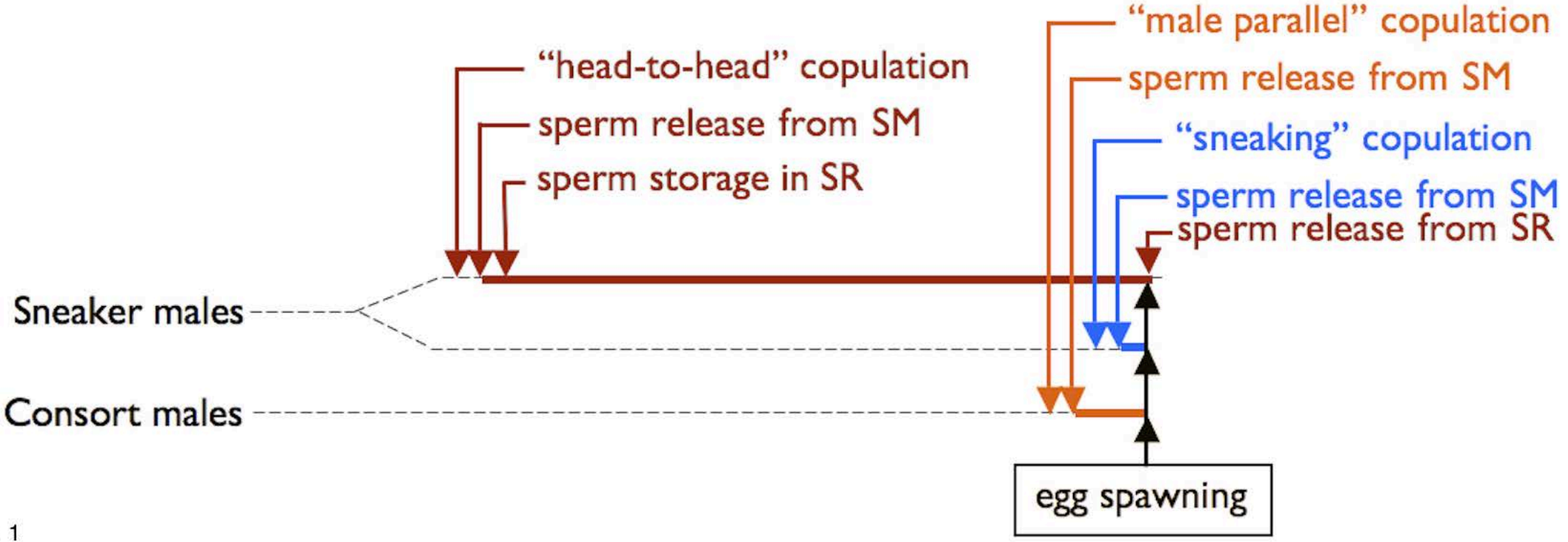
"male parallel" copulation
sperm release from SM
"head-to-head" copulation
"sneaking" copulation
sperm release from SM
sperm release from SM
sperm storage in SR
sperm release from SR
Sneaker males
Consort males
egg spawning

Fig. 1

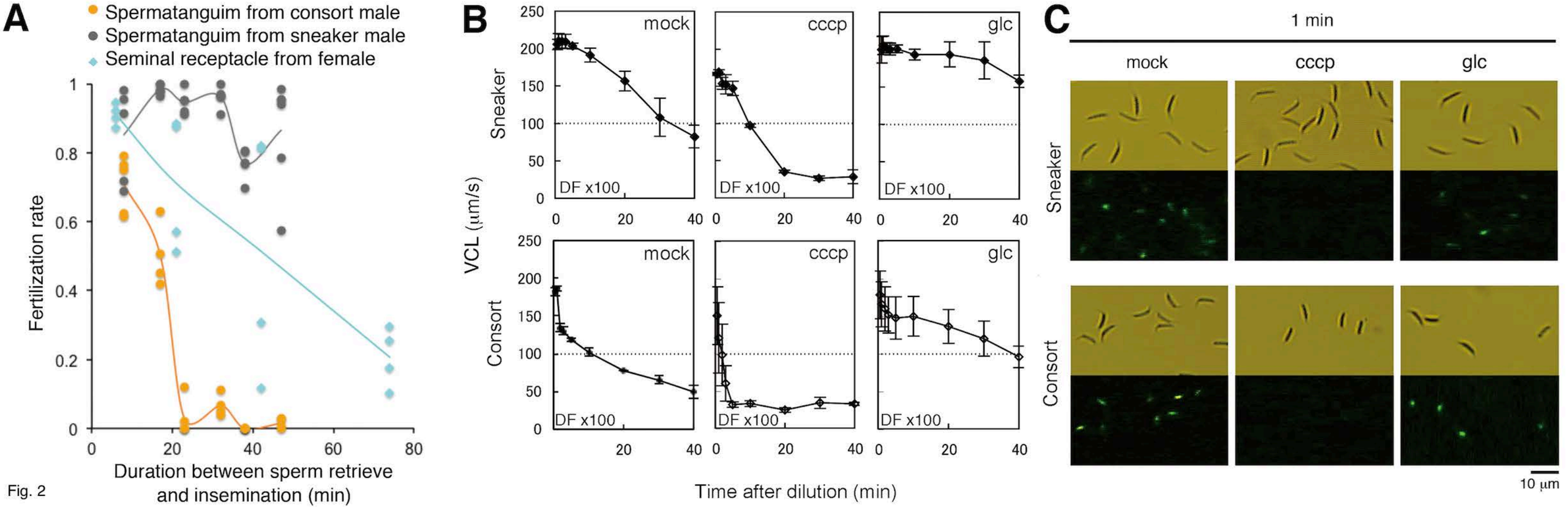
A
Spermatanguim from consort male
Spermatanguim from sneaker male
Seminal receptacle from female
Fertilization rate
Duration between sperm retrieve and insemination (min)
B
mock
cccp
glc
Sneaker
Consort
DF x100
VCL (μm/s)
Time after dilution (min)
C
1 min
mock
cccp
glc
Sneaker
Consort
10 μm

Fig. 2

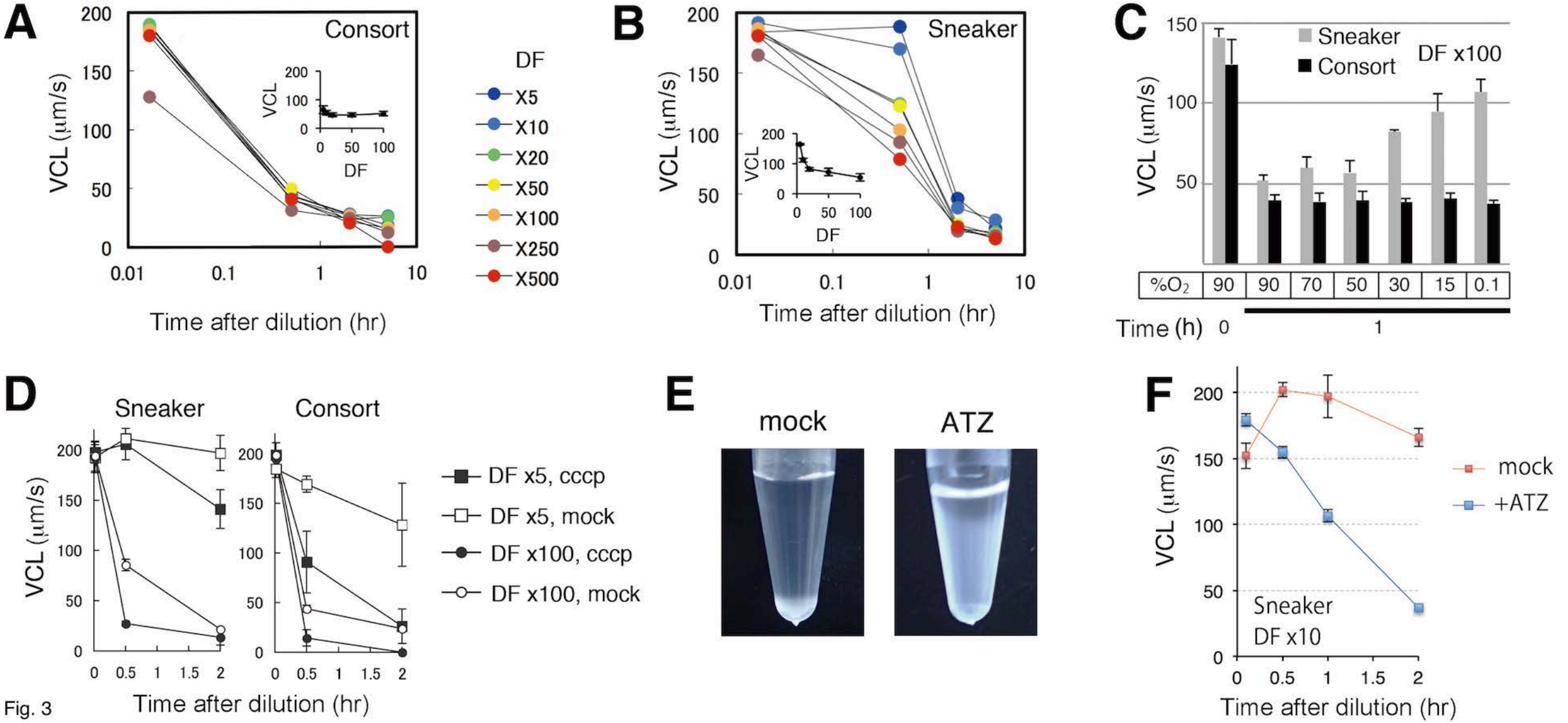
A
Consort
VCL (μm/s)
Time after dilution (hr)
DF
X5
X10
X20
X50
X100
X250
X500
B
Sneaker
C
Sneaker
Consort
DF x100
%O2
90
90
70
50
30
15
0.1
Time (h)
0
1
D
Sneaker
Consort
DF x5, cccp
DF x5, mock
DF x100, cccp
DF x100, mock
E
mock
ATZ
F
mock
+ATZ
Sneaker
DF x10

Fig. 3

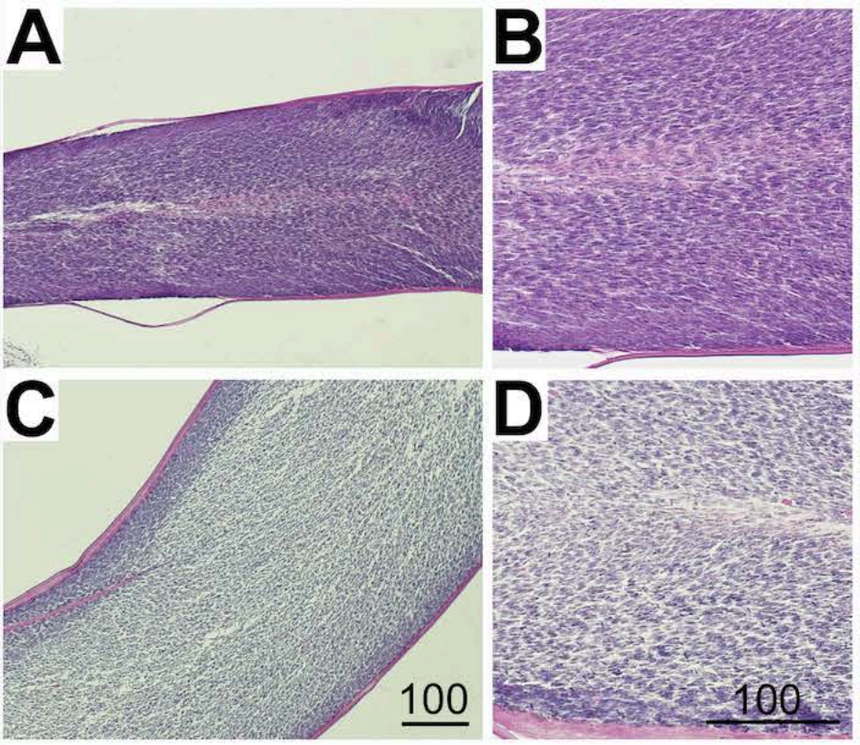
A
B
C
D
100
100

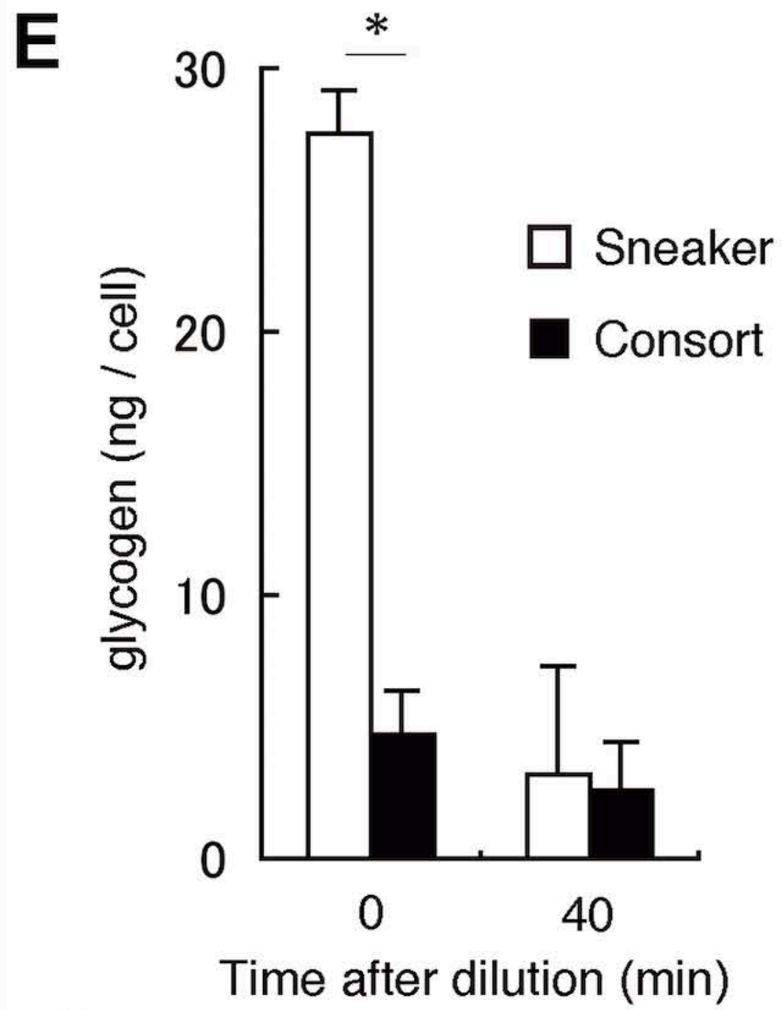
E
30
20
10
0
glycogen (ng / cell)
*
Sneaker
Consort
0
40
Time after dilution (min)


F
Nuc
Mito
Fla
3

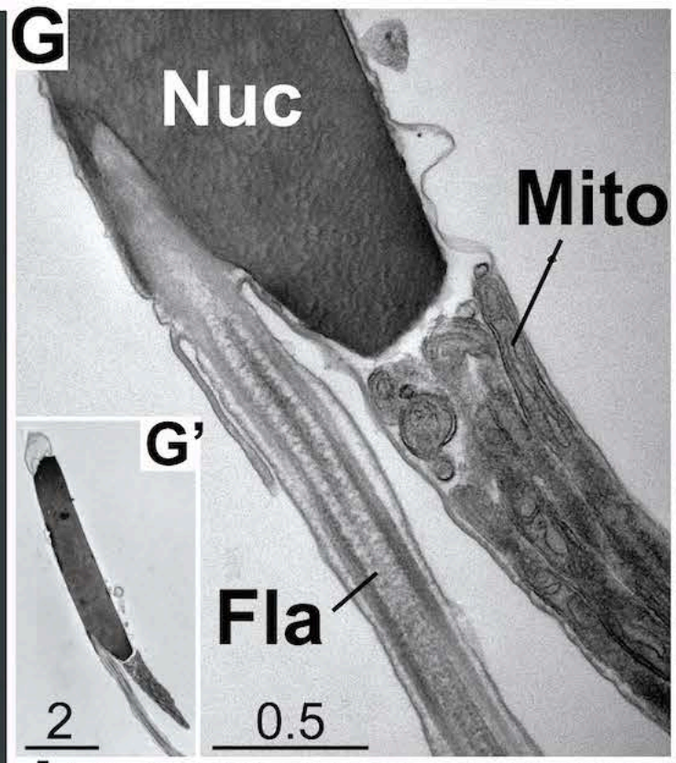
G
Nuc
Mito
Fla
0.5
G'
2

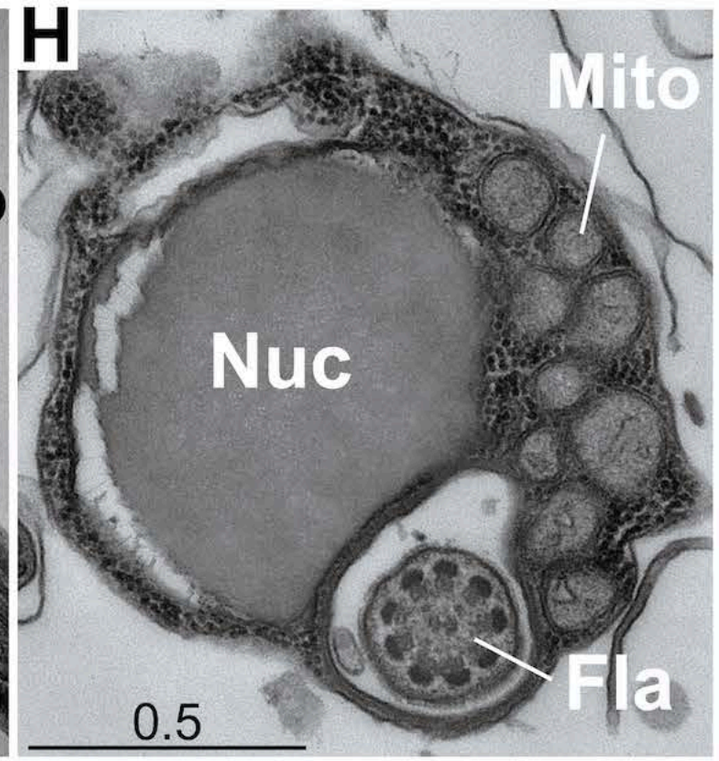
H
Mito
Nuc
Fla
0.5

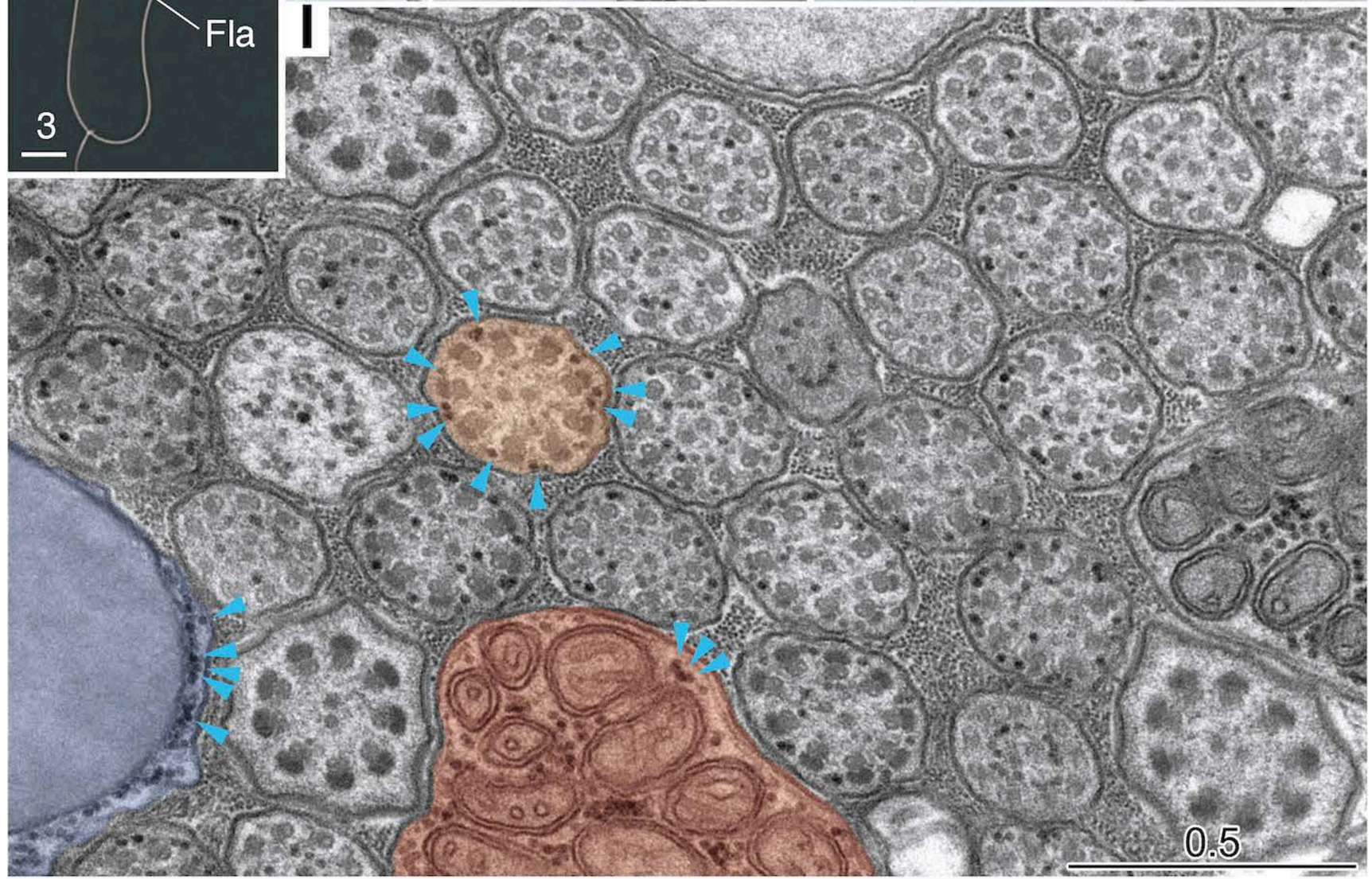
I
0.5

Fig. 4

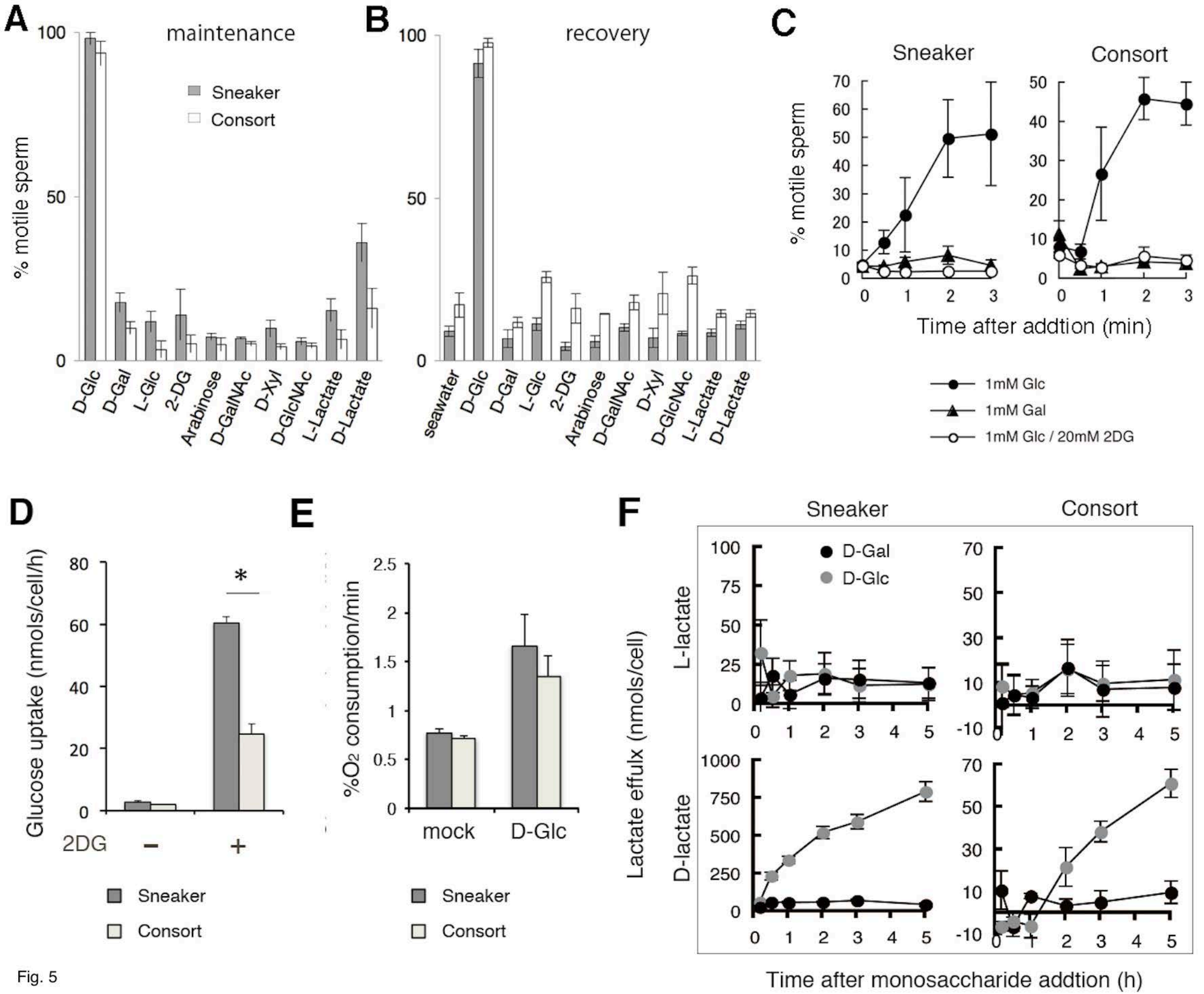
A
maintenance
Sneaker
Consort
% motile sperm
100
50
0
D-Glc
D-Gal
L-Glc
2-DG
Arabinose
D-GalNAc
D-Xyl
D-GlcNAc
L-Lactate
D-Lactate
B
recovery
seawater
C
Sneaker
Consort
% motile sperm
Time after addtion (min)
1mM Glc
1mM Gal
1mM Glc / 20mM 2DG
D
Glucose uptake (nmols/cell/h)
2DG
Sneaker
Consort
E
%O2 consumption/min
mock
D-Glc
F
D-Gal
D-Glc
L-lactate
D-lactate
Lactate effulx (nmols/cell)
Time after monosaccharide addtion (h)

Fig. 5

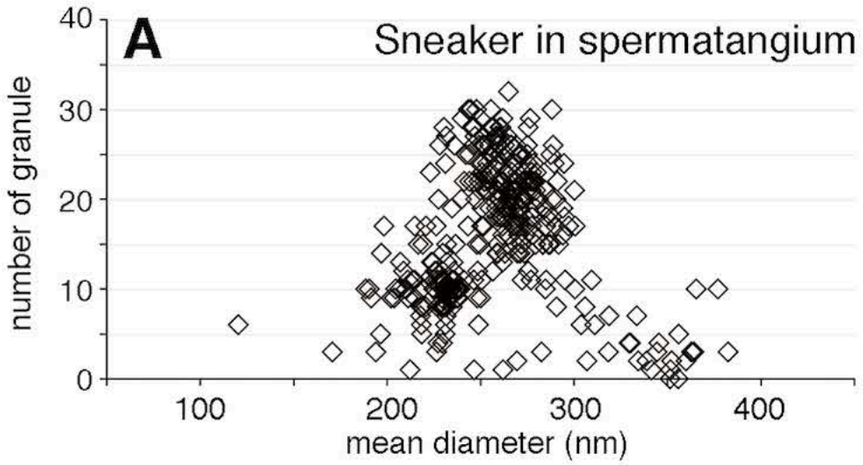
A
Sneaker in spermatangium
number of granule
mean diameter (nm)

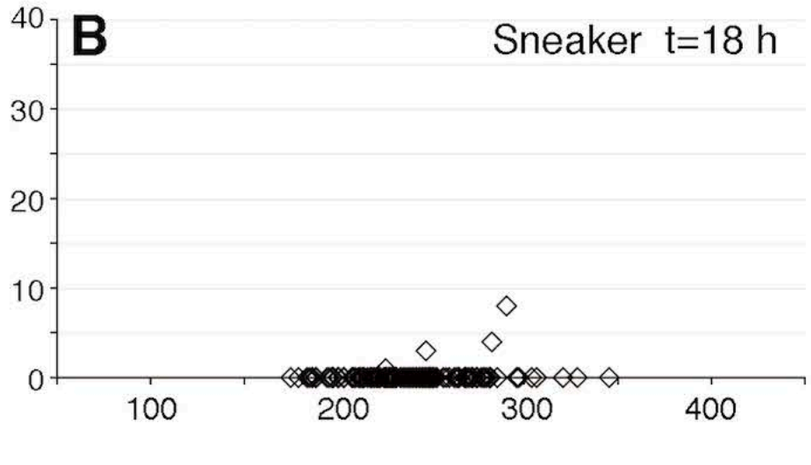
B
Sneaker t=18 h

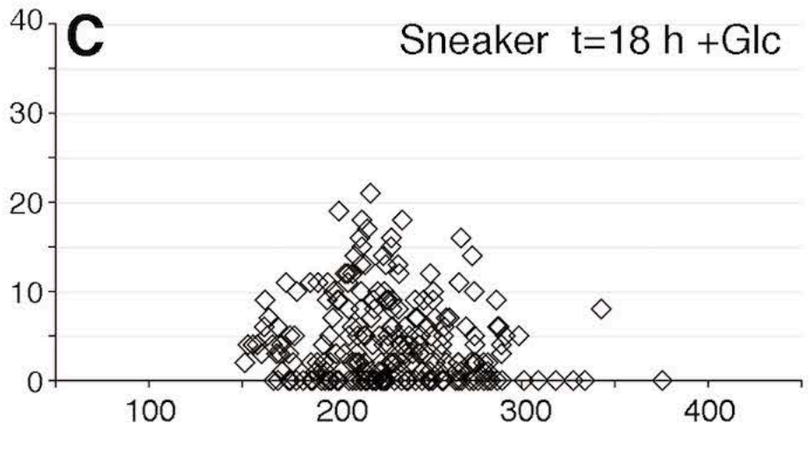
C
Sneaker t=18 h +Glc

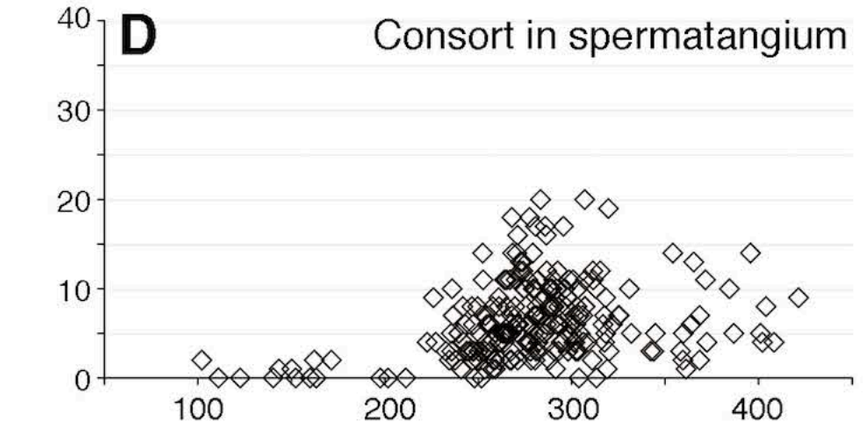
D
Consort in spermatangium

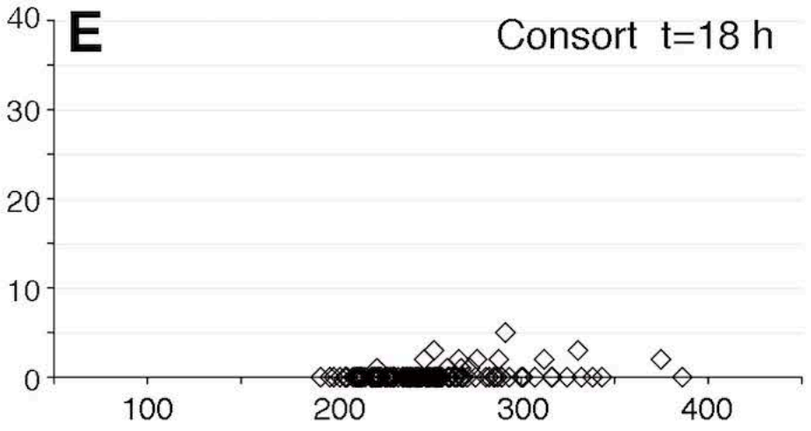
E
Consort t=18 h

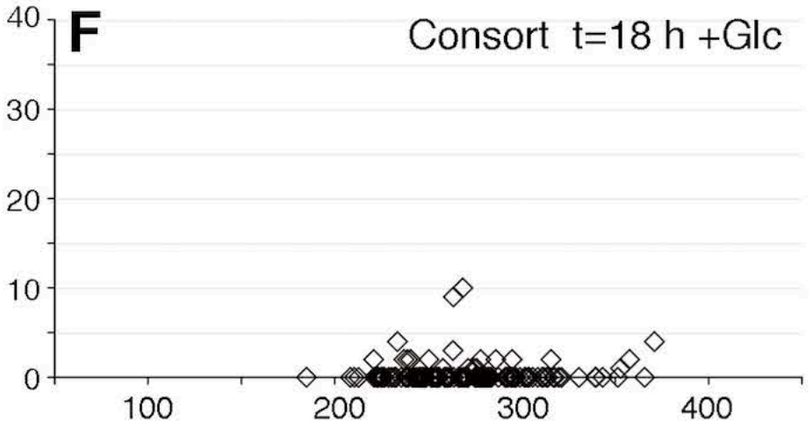
F
Consort t=18 h +Glc

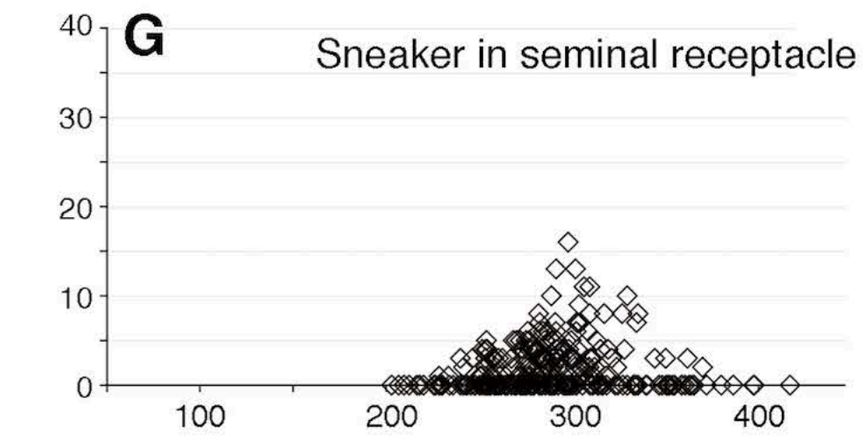
G
Sneaker in seminal receptacle

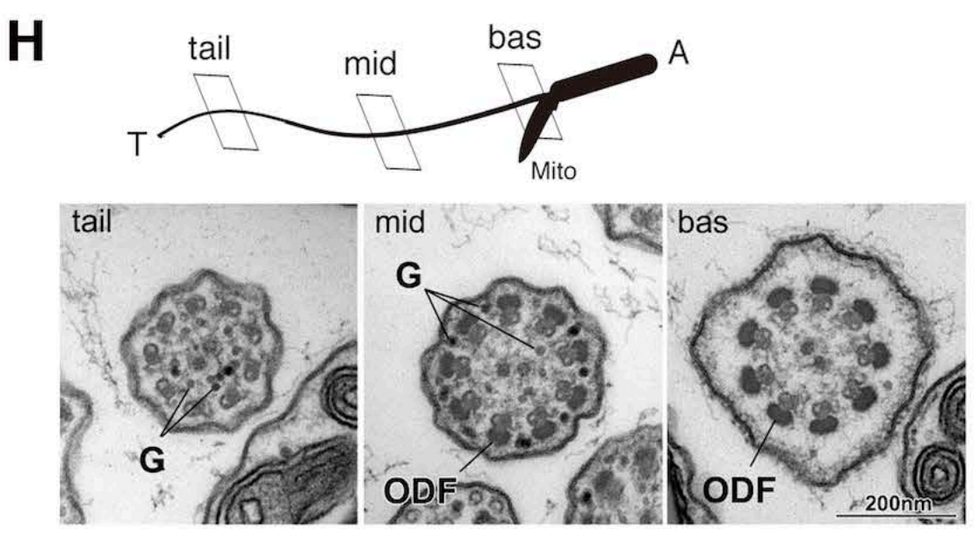
H
tail
mid
bas
A
T
Mito
tail
G
mid
G
ODF
bas
ODF
200nm

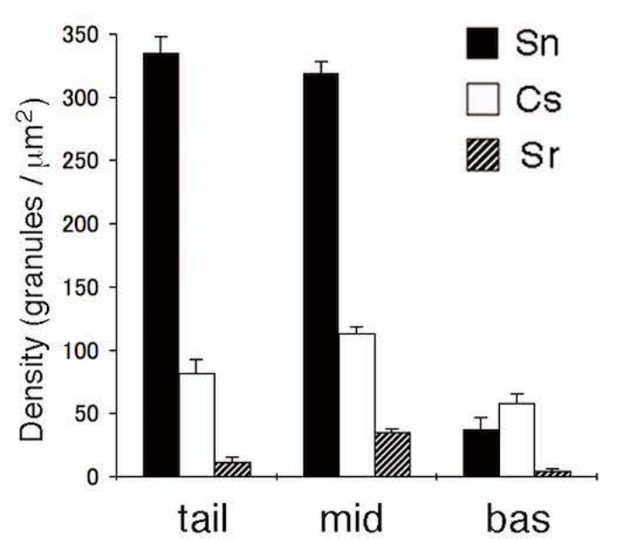
I
Sn
Cs
Sr
Density (granules / μm2)
tail
mid
bas

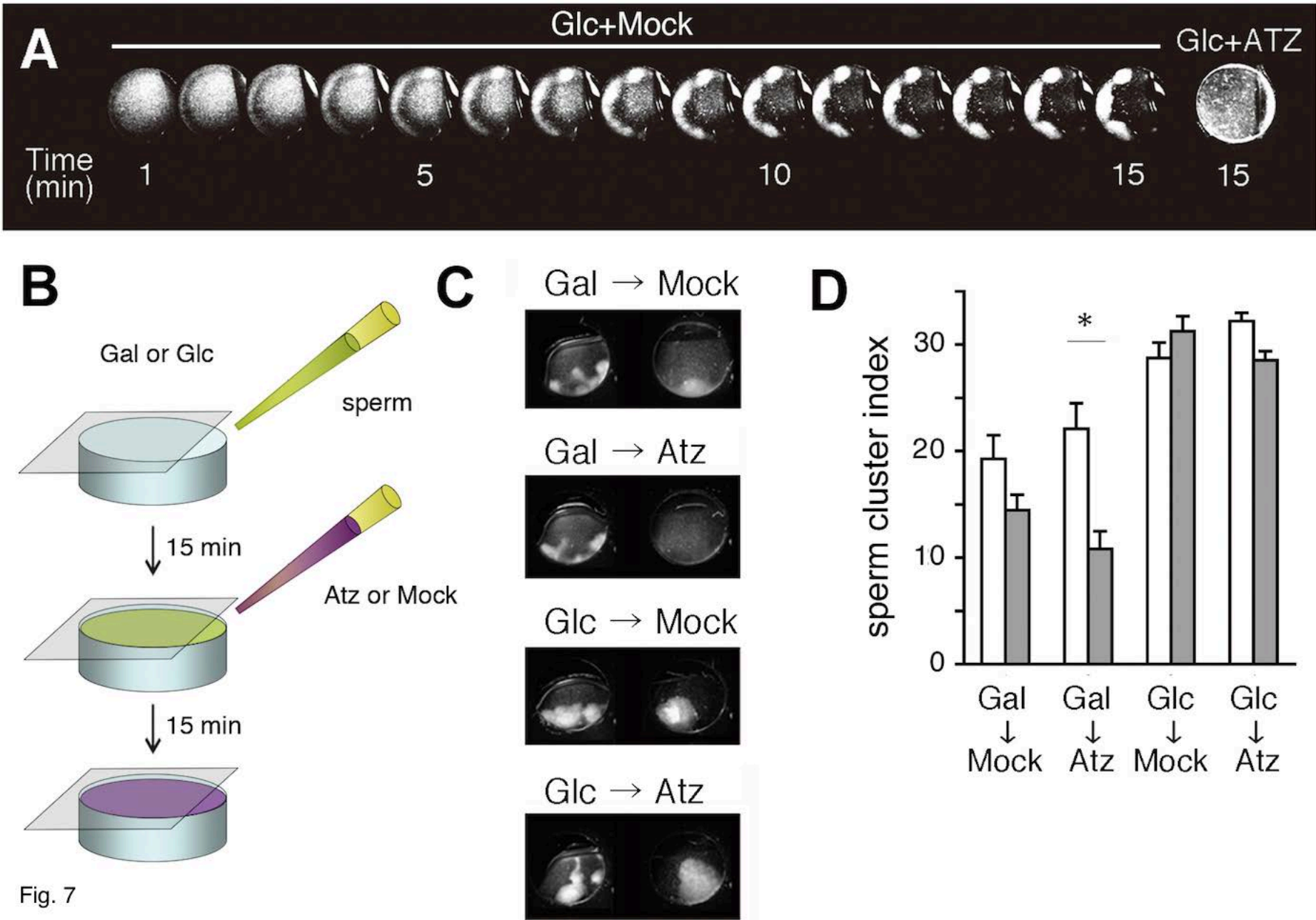
A
Glc+Mock
Glc+ATZ
Time (min)
1
5
10
15
15
B
Gal or Glc
sperm
15 min
Atz or Mock
15 min
C
Gal → Mock
Gal → Atz
Glc → Mock
Glc → Atz
D
sperm cluster index
0
10
20
30
*
Gal ↓ Mock
Gal ↓ Atz
Glc ↓ Mock
Glc ↓ Atz

Fig. 7

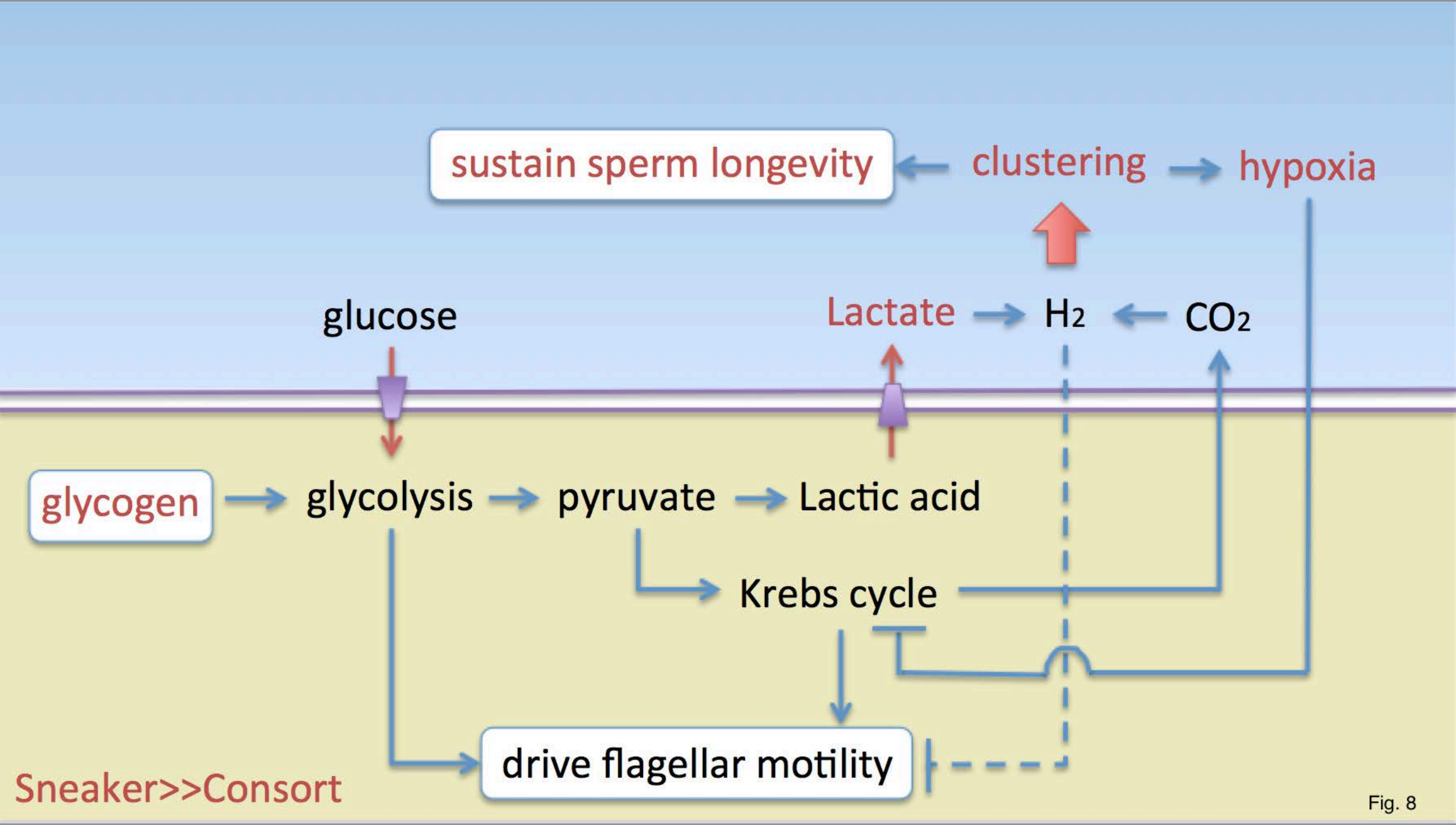
sustain sperm longevity
clustering
hypoxia
glucose
Lactate
H2
CO2
glycogen
glycolysis
pyruvate
Lactic acid
Krebs cycle
drive flagellar motility
Sneaker>>Consort

Fig. 8